Laminar heat transfer in concentric annuli with viscous dissipation and fluid axial heat conduction (Part I: Thermal boundary condition of the first kind)

by

Ganbat DAVAA*, Toru SHIGECHI**, Satoru MOMOKI** and Odgerel JAMBAL*

The present numerical study investigates the influence of fluid axial heat conduction, viscous dissipation, relative velocity of the core and radius ratio on laminar heat transfer in a concentric annular duct with a moving boundary. The solution is based on coordinate transformation of the elliptic energy equation. The temperature distributions of non-Newtonian fluids for infinite extend ($-\infty < z < \infty$) were determined by solving the energy equation including the viscous dissipation term and the fluid axial heat conduction term subject to the constant wall temperature boundary condition. The effects of radius ratio, relative core velocity, flow index, dimensionless shear rate parameter, Brinkman number and Peclet number on the developing temperature distribution and Nusselt number at the walls are discussed.

1. Introduction

We consider thermally developing and hydrodynamically developed laminar flow of non-Newtonian fluids flowing in annuli with axially moving cores. The emphasis in this study is on investigating the effects of viscous dissipation, fluid axial heat conduction, relative velocity of the moving core, flow index and the radius ratio of the annuli on the developing heat transfer.

In the previous study[1], the developing heat transfer problem was analyzed by neglecting fluid axial heat conduction effects. Without the fluid axial heat conduction term, the familiar Graetz problem of laminar heat transfer in a conduit is simplified from an elliptic type problem to a parabolic one. In the previous work[1], the parabolic energy equation including the viscous dissipation term was solved numerically for the first and second kinds of thermal boundary conditions by applying velocity profiles presented in the previous report[2] for modified power-law fluids.

It is the aim of this work to clarify the combined effects of viscous dissipation, fluid axial heat conduction, relative velocity of the core, flow index and radius ratio on the developing thermal entrance heat transfer of non-Newtonian fluids. In this paper the results of the study on the developing heat transfer subject to the thermal boundary condition of constant wall temperature are presented. The effect of viscous dissipation is estimated by the magnitude of Brinkman number. Peclet number is introduced to serve as a controlling index that indicates the effect of fluid axial heat conduction. Therefore the problem is controlled by the magnitudes of Brinkman number, which represents the ratio of overall dissipation to wall heat transfer, Peclet number, which characterizes the ratio of axial heat convection to axial heat conduction, dimensionless relative velocity of the moving core, which is the ratio of the moving core velocity to the average velocity of the fluid, radius ratio and rheological parameters such as flow index and dimensionless shear rate parameter.

In this study, the conduit is considered in two semi-infinite regions $-\infty < z < 0$ and $0 \leq z < \infty$. The two semi-infinite regions are necessary to be considered for the investigation on the fluid axial heat conduction because in reality the temperature profile of the fluid at $z = 0$ (where wall heating commences) is affected by fluid axial heat conduction from downstream.

Nomenclature

Br	Brinkman number
c_p	specific heat at constant pressure, [J/(kg·K)]
D_h	hydraulic diameter $\equiv 2(R_o - R_i)$, [m]
E	constant of the axial transformation

Received on October 25, 2002
* Graduate School of Science and Technology
** Department of Mechanical Systems Engineering

h heat transfer coefficient, [W/(m^2 K)]
k thermal conductivity, [W/(m· K)]
m consistency index, [N · s^n/m^2]
n flow index
Nu Nusselt number
Pe Peclet number
Pr_{M} modified Prandtl number
r radial coordinate, [m]
r^* dimensionless radial coordinate $\equiv r/D_{\mathrm{h}}$
R radius, [m]
Re_{M} modified Reynolds number
T temperature, [K]
u velocity of the fluid, [m/s]
u_{m} average velocity of the fluid, [m/s]
u^* dimensionless velocity $\equiv u/u_{\mathrm{m}}$
U axial velocity of the moving core, [m/s]
U^* dimensionless relative velocity of the moving core $\equiv U/u_{\mathrm{m}}$
z axial coordinate, [m]
z^* dimensionless axial coordinate $\equiv z/(PeD_{\mathrm{h}})$
z_t transformed axial coordinate

Greek Symbols

α radius ratio $\equiv R_{\mathrm{i}}/R_{\mathrm{o}}$
β dimensionless shear rate parameter
η_a apparent viscosity, [kg/(m· s)]
η_a^* dimensionless apparent viscosity $\equiv \eta_a/\eta^*$
η_0 viscosity at zero shear rate, [kg/(m· s)]
η^* reference viscosity, [kg/(m· s)]
ρ density, [kg/m^3]
θ dimensionless temperature
ξ transformed dimensionless radial coordinate $\equiv [2(1-\alpha)r^* - \alpha]/(1-\alpha)$

Subscripts

b bulk
e entrance
fd fully developed
i inner tube or core
o outer tube

2. Analysis

The physical model for the analysis is shown in Fig.1. The core tube moves axially at a constant velocity, U. The assumptions and conditions used in the analysis are:

- The flow is incompressible, steady-laminar, and fully developed hydrodynamically.
- The fluid is non-Newtonian and the shear stress may be described by the modified power-law model[3], and physical properties are constant except viscosity.

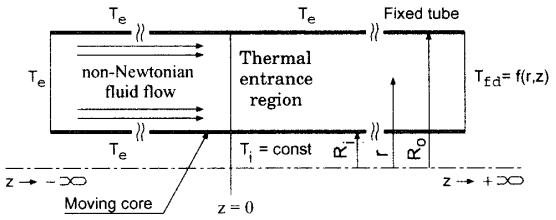

Fig.1 Schematic of a concentric annulus with an axially moving core

- The body forces are neglected.
- The entering fluid temperature, T_e, is uniform at upstream infinity ($z \to -\infty$) and the outer tube wall temperature is equal to T_e everywhere. The core is kept at a constant temperature $T_e < T_{\mathrm{i}}$ for $0 \le z$, whereas for $z < 0$ the temperature is equal to T_e.

The energy equation together with the assumptions above is written as

$$k\left[\frac{1}{r}\frac{\partial}{\partial r}\left(r\frac{\partial T}{\partial r}\right)+\frac{\partial^2 T}{\partial z^2}\right]+\eta_a\left(\frac{du}{dr}\right)^2=\rho c_{\mathrm{p}} u\frac{\partial T}{\partial z} \quad (1)$$

$$\text{in} \quad R_{\mathrm{i}} \le r \le R_{\mathrm{o}} \quad \text{and} \quad -\infty \le z \le \infty$$

$$\begin{cases} T = T_e & \text{at} \quad r = R_{\mathrm{i}} & 0 \le z \\ T = T_{\mathrm{i}} & \text{at} \quad r = R_{\mathrm{o}} & 0 \le z \\ T = T_e & \text{at} \quad r = R_{\mathrm{i}} & z < 0 \\ T = T_e & \text{at} \quad r = R_{\mathrm{o}} & z < 0 \\ T = T_e & \text{at} \quad R_{\mathrm{i}} \le r \le R_{\mathrm{o}} & z \to -\infty \\ T = T_{fd} & \text{at} \quad R_{\mathrm{i}} \le r \le R_{\mathrm{o}} & z \to +\infty \end{cases} \quad (2)$$

The velocity, u, and its gradient, $\frac{du}{dr}$, have been obtained in the previous report[2].
Bulk temperature and Nusselt number are defined as

$$T_{\mathrm{b}} \equiv \frac{2}{u_{\mathrm{m}}\left(R_{\mathrm{o}}^2 - R_{\mathrm{i}}^2\right)}\int_{R_{\mathrm{i}}}^{R_{\mathrm{o}}} uTr\, dr \quad (3)$$

$$Nu \equiv \frac{hD_{\mathrm{h}}}{k} \quad (4)$$

Heat transfer coefficients are:

$$h_{\mathrm{i}} = \frac{-k\frac{\partial T}{\partial r}\Big|_{r=R_{\mathrm{i}}}}{T_{\mathrm{i}} - T_{\mathrm{b}}} \qquad h_{\mathrm{o}} = \frac{k\frac{\partial T}{\partial r}\Big|_{r=R_{\mathrm{o}}}}{T_{\mathrm{o}} - T_{\mathrm{b}}} \quad (5)$$

The following dimensionless variables are introduced

$$r^* = \frac{r}{D_h} \qquad z^* = \frac{z}{PeD_h} \tag{6}$$

$$u^* = \frac{u}{u_m} \qquad \beta = \frac{\eta_0}{m}\left(\frac{u_m}{D_h}\right)^{1-n} \tag{7}$$

$$\alpha = \frac{R_i}{R_o} \qquad \theta = \frac{T - T_e}{T_i - T_e} \tag{8}$$

where

$$Pe = Re_M \cdot Pr_M \tag{9}$$

$$Re_M \equiv \frac{\rho u_m D_h}{\eta^*} \qquad Pr_M \equiv \frac{c_p \eta^*}{k} \tag{10}$$

$$Br = \eta^* \frac{u_m^2}{k\,(T_i - T_e)} \tag{11}$$

With the substitution of the above quantities into the dimensional formulation, the dimensionless energy equation and boundary conditions are obtained as

$$\frac{1}{r^*}\frac{\partial}{\partial r^*}\left(r^*\frac{\partial\theta}{\partial r^*}\right) + \frac{1}{Pe^2}\frac{\partial^2\theta}{\partial z^{*2}} + Br\cdot\eta_a^*\left(\frac{du^*}{dr^*}\right)^2 = u^*\frac{\partial\theta}{\partial z^*} \tag{12}$$

in $\frac{\alpha}{2(1-\alpha)} \le r^* \le \frac{1}{2(1-\alpha)}$ and $-\infty \le z^* \le \infty$

$$\begin{cases} \theta = 1 \text{ at } r^* = \frac{\alpha}{2(1-\alpha)} & 0 \le z^* \\ \theta = 0 \text{ at } r^* = \frac{1}{2(1-\alpha)} & 0 \le z^* \\ \theta = 0 \text{ at } r^* = \frac{\alpha}{2(1-\alpha)} & z^* < 0 \\ \theta = 0 \text{ at } r^* = \frac{1}{2(1-\alpha)} & z^* < 0 \\ \theta = 0 \text{ at } \frac{\alpha}{2(1-\alpha)} \le r^* \le \frac{1}{2(1-\alpha)} & z^* = -\infty \\ \theta = \theta_{fd} \text{ at } \frac{\alpha}{2(1-\alpha)} \le r^* \le \frac{1}{2(1-\alpha)} & z^* = +\infty \end{cases} \tag{13}$$

For infinitely large values of the axial distance ($z^* \to \infty$), the terms $\frac{\partial^2\theta}{\partial z^{*2}}$ and $\frac{\partial\theta}{\partial z^*}$ vanish. Then the dimensionless temperature θ_{fd} corresponding to the boundary condition of constant wall temperature is the particular solution of the following equation:

$$\frac{1}{r^*}\frac{\partial}{\partial r^*}\left(r^*\frac{\partial\theta_{df}}{\partial r^*}\right) = -Br\cdot\eta_a^*\left(\frac{du^*}{dr^*}\right)^2 \tag{14}$$

$$\begin{cases} \theta = 1 \text{ at } r^* = \frac{\alpha}{2(1-\alpha)} \\ \theta = 0 \text{ at } r^* = \frac{1}{2(1-\alpha)} \end{cases} \tag{15}$$

Bulk temperature in the dimensionless form:

$$\theta_b = \frac{8(1-\alpha)}{1+\alpha}\int_{\frac{\alpha}{2(1-\alpha)}}^{\frac{1}{2(1-\alpha)}} u^*\theta r^*\, dr^* \tag{16}$$

Then Nu at the walls are

$$Nu_i = -\frac{1}{(\theta_i - \theta_b)}\left.\frac{\partial\theta}{\partial r^*}\right|_{\frac{\alpha}{2(1-\alpha)}} \tag{17}$$

$$Nu_o = \frac{1}{(\theta_o - \theta_b)}\left.\frac{\partial\theta}{\partial r^*}\right|_{\frac{1}{2(1-\alpha)}} \tag{18}$$

3. Numerical calculation

In order to convert the upstream and downstream infinities, the dimensionless axial coordinate z^* is transformed according to the relation employed by Verhoff and Fisher[4] as follows:

$$z^* = E\tan(\pi z_t) \quad \text{or} \quad z_t = \frac{1}{\pi}\arctan\frac{z^*}{E} \tag{19}$$

By introducing the transformed coordinate z_t, the energy equation and the boundary conditions become

$$\frac{\partial^2\theta}{\partial r^{*2}} + B\frac{\partial^2\theta}{\partial z_t^2} + \frac{1}{r^*}\frac{\partial\theta}{\partial r^*} + Br\cdot\eta_a^*\left(\frac{du^*}{dr^*}\right)^2 = A\frac{\partial\theta}{\partial z_t} \tag{20}$$

$$\text{in} \quad \frac{\alpha}{2(1-\alpha)} \le r^* \le \frac{1}{2(1-\alpha)} \quad \text{and}$$

$$-0.5 \le z_t \le 0.5$$

where

$$A = \frac{\cos^2(\pi z_t)}{\pi E}\left[u^* + \frac{1}{Pe^2}\frac{\sin(2\pi z_t)}{E}\right] \tag{21}$$

$$B = \frac{1}{Pe^2}\left[\frac{\cos^2(\pi z_t)}{\pi E}\right]^2 \tag{22}$$

$$\begin{cases} \theta = 1 \text{ at } r^* = \frac{\alpha}{2(1-\alpha)}, & 0 \le z_t \le 0.5 \\ \theta = 0 \text{ at } r^* = \frac{1}{2(1-\alpha)}, & 0 \le z_t \le 0.5 \\ \theta = 0 \text{ at } r^* = \frac{\alpha}{2(1-\alpha)}, & -0.5 \le z_t < 0 \\ \theta = 0 \text{ at } r^* = \frac{1}{2(1-\alpha)}, & -0.5 \le z_t < 0 \\ \theta = 0 \text{ at } \frac{\alpha}{2(1-\alpha)} \le r^* \le \frac{1}{2(1-\alpha)} & z^* = -0.5 \\ \theta = \theta_{fd} \text{ at } \frac{\alpha}{2(1-\alpha)} \le r^* \le \frac{1}{2(1-\alpha)} & z^* = 0.5 \end{cases} \tag{23}$$

Equations (14) and (20) along with the associated boundary conditions have been solved numerically. The solution zone was laid in the range of $\alpha/[2(1-\alpha)] \leq r^* \leq 1/[2(1-\alpha)]$ and $-0.5 \leq z_t \leq +0.5$. The numerical approach employed for the system equations was based on Gauss-Seidel method. An irregular mesh system consisting of denser grids near $z_t = 0$ was applied to allow more accurate representation of the fluid axial heat conduction effect. The finest mesh was used next to $z_t = 0$ and as the location of the node goes farther from the origin, mesh size is increased with a ratio $\Delta z_n/\Delta z_{n-1}$. Along the radial axis the solution zone was divided evenly. The calculation has been carried out with two steps in order to get the results with a high accuracy. First, the temperature at every node within the whole calculation zone in which z^* ranges in between $-\infty$ to $+\infty$ has been calculated. Then by using the calculation results of the temperature at $z^* = 0.0$ and $z^* = 1.001$, more accurately calculated temperature profiles at the thermally developing region have been obtained. In the first step the finest mesh spacing was $\Delta z = 1.059 \cdot 10^{-7}$ and, mesh size was changed with the ratio $\Delta z_{n-1}/\Delta z_n = 1.33$ for $z_t \leq 0$ and $\Delta z_n/\Delta z_{n-1} = 1.33$ for $0 \leq z_t$. In the second step, the finest mesh spacing was $\Delta z = 4.93 \cdot 10^{-7}$ and the ratio was $\Delta z_n/\Delta z_{n-1} = 1.02$. Constant of the axial transformation, E, was chosen as 4.62 in the both calculation steps.

4. Results and discussion

Temperature distributions of non-Newtonian fluids for $-\infty < z < \infty$ in concentric annuli with moving cores were calculated for the boundary condition of constant wall temperature. The calculation has been carried out by using the finite difference method. The following range of parameters are considered for Newtonian ($n = 1$), pseudoplastic ($n = 0.5$, $\beta = 1$) and dilatant ($n = 1.5$, $\beta = 1$) fluids in order to study the effects of viscous dissipation, fluid axial heat conduction, geometry of the annuli, and moving boundary:

Brinkman number: 0.0, 0.01, 0.05 and 0.1

Peclet number: ∞, 100, 50, 20, 10, 5 and 1

Radius ratio: 0.2, 0.5 and 0.8

The relative velocity: 0 and 1.

The case with $Br = 0.0$ and $Pe \to \infty$ is the limiting case of neglected viscous dissipation and axial heat conduction. It is worthwhile, to compare the results of Newtonian fluids whose predictions were for stationary wall boundaries[5] ($U^* = 0$) and by Shigechi and Araki[6] for the moving boundary ($U^* = 1.0$) case, respectively. It can be seen in Fig.2 even at small values of z^*, the agreement is excellent.

It is also seen that, the change in Nu at the thermal entrance region (for small z^*) becomes rather not rapid if Pe is small. The same trend was observed for Newtonian and non-Newtonian fluid flows. This behavior is attributed to that the fluid temperature increases due to axial heat conduction (at $z \leq 0$) before the fluid enters into the heated wall region. This effect of fluid axial heat conduction is shown obviously in Figs.3 and 4 which illustrate respectively developing temperature profiles of a pseudoplastic fluid ($\alpha = 0.5$, $n = 0.5$ and $\beta = 1$) for cases of the stationary core and the moving core.

For $Pe = 10$ the fluid temperature increase is occurred at negative values of z^*. For $Pe \to \infty$ even at $z^* = 0$, where the step change in wall temperature, the dimensionless temperature of the fluid is zero except the cases with considerable viscous dissipation. This indicates the vanishing influence of axial heat conduction in the fluid for $z^* \leq 0$ with an increasing Peclet number.

For $Br = 0.0$ fluid is considered as it experiences no gain of heat due to viscous dissipation. For larger values of Br, it can be seen that the dimensionless temperature of the fluid at $z^* \leq 0$ deviates significantly from zero. This increase is due to the contribution of viscous dissipation to the flowing fluid.

Since the highest shear rate occurs near the stationary tube, the effect of viscous dissipation is most significant near the fixed tube and it is seen that the temperature increase due to viscous dissipation is greater for $U^* = 0$.

For the case of the stationary core, the increase of temperature of the fluid due to fluid axial heat conduction and viscous dissipation is higher than in the case of moving boundary. It is seen as soon as z^* becomes positive the fluid temperature profile undergoes rather rapid change causing a decrease in Nu at the core.

Figures 5 and 6 compare the profiles of bulk temperature and Nusselt numbers at the tubes for the cases of the stationary core and the moving core. The presented profiles are the calculation results for various Peclet number with $Br = 0.1$. The fluids under consideration are a pseudoplastic fluid and a dilatant fluid respectively in these figures. The radius ratio of the annulus under consideration is 0.5. It can be observed that the asymptotic Nusselt number profiles are identical

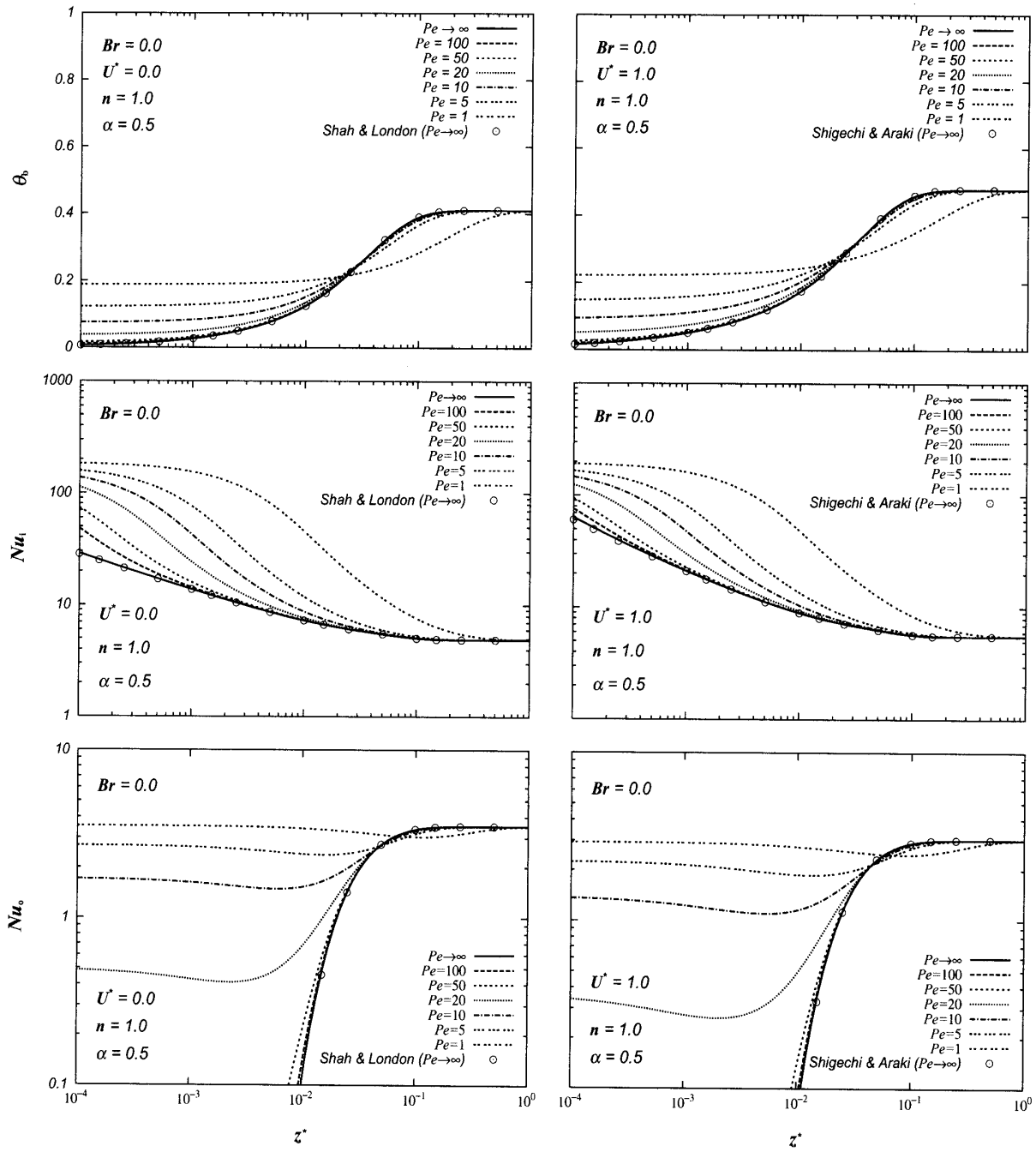

Fig.2 θ_b and Nu for a Newtonian fluid, $Br = 0.0$ ($U^* = 0$ and $U^* = 1$)

for all Pe values. The figures indicate that Pe does not effect on Nu at a location farther downstream and, Nu at the tubes remains fairly uniform throughout the thermal entrance region specially for small z^* if Pe is moderate. It also can be explained that, the fluid temperature increases due to fluid axial heat conduction. Including fluid axial heat conduction causes an increase in Nusselt number at the core tube whose temperature is higher than the entering fluid temperature. For a specified axial position Nusselt number at the moving core ($U^* = 1$) is larger than the corresponding Nusselt number at the fixed core ($U^* = 0$) with the given Brinkman number and Peclet number if the fluid is a pseudoplastic fluid.

In view of combined effects of viscous dissipation, fluid axial heat conduction, radius ratio, flow index and the relative velocity of the moving core on the developing heat transfer, it is desirable to present the heat transfer results for the case of the stationary core and the moving core with the various corresponding parameters. From Figs.7 and

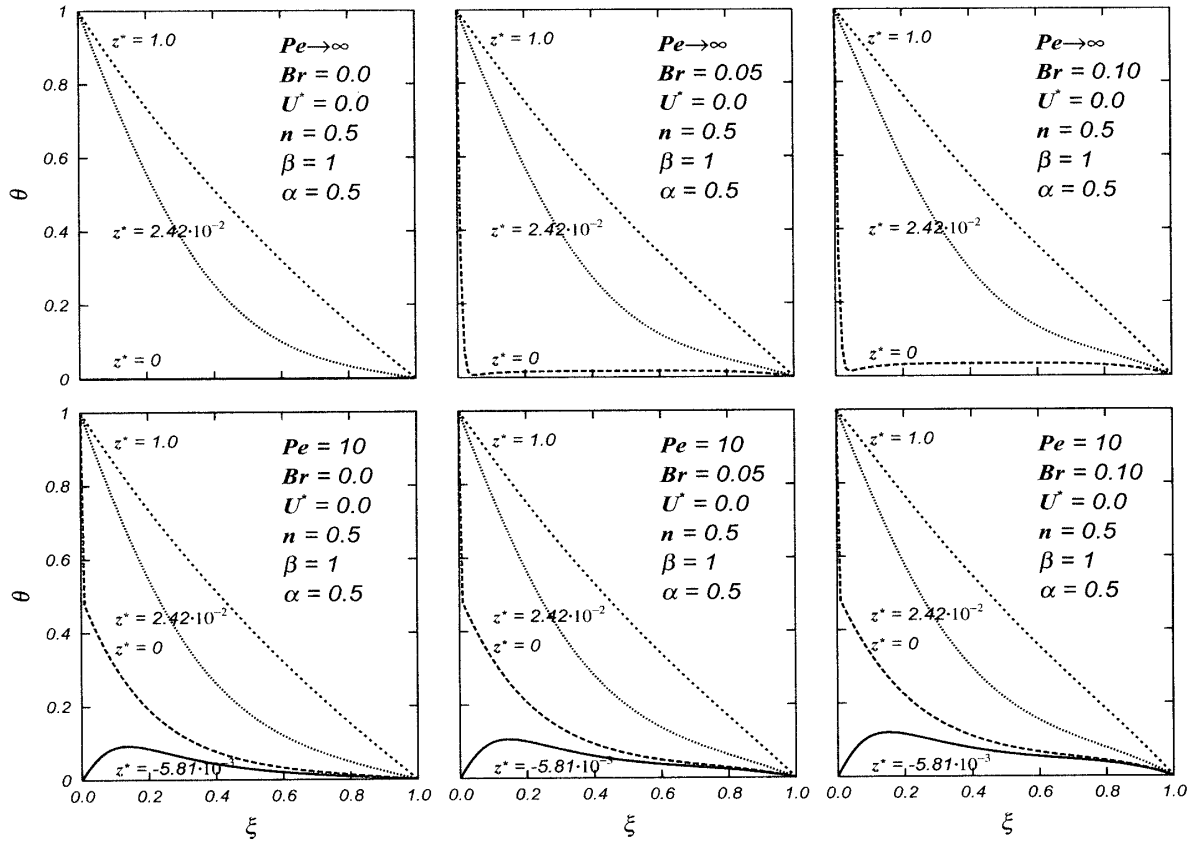

Fig.3 Developing temperature profiles ($U^* = 0$)

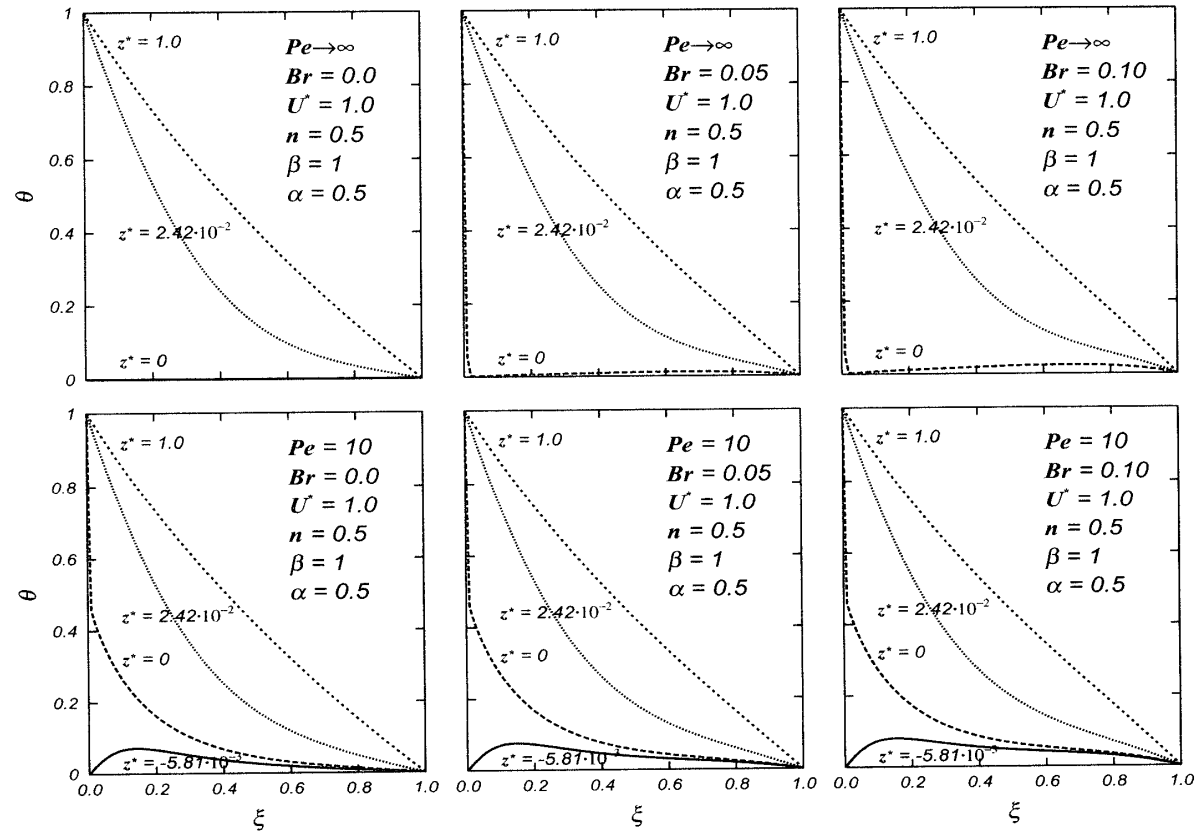

Fig.4 Developing temperature profiles ($U^* = 1$)

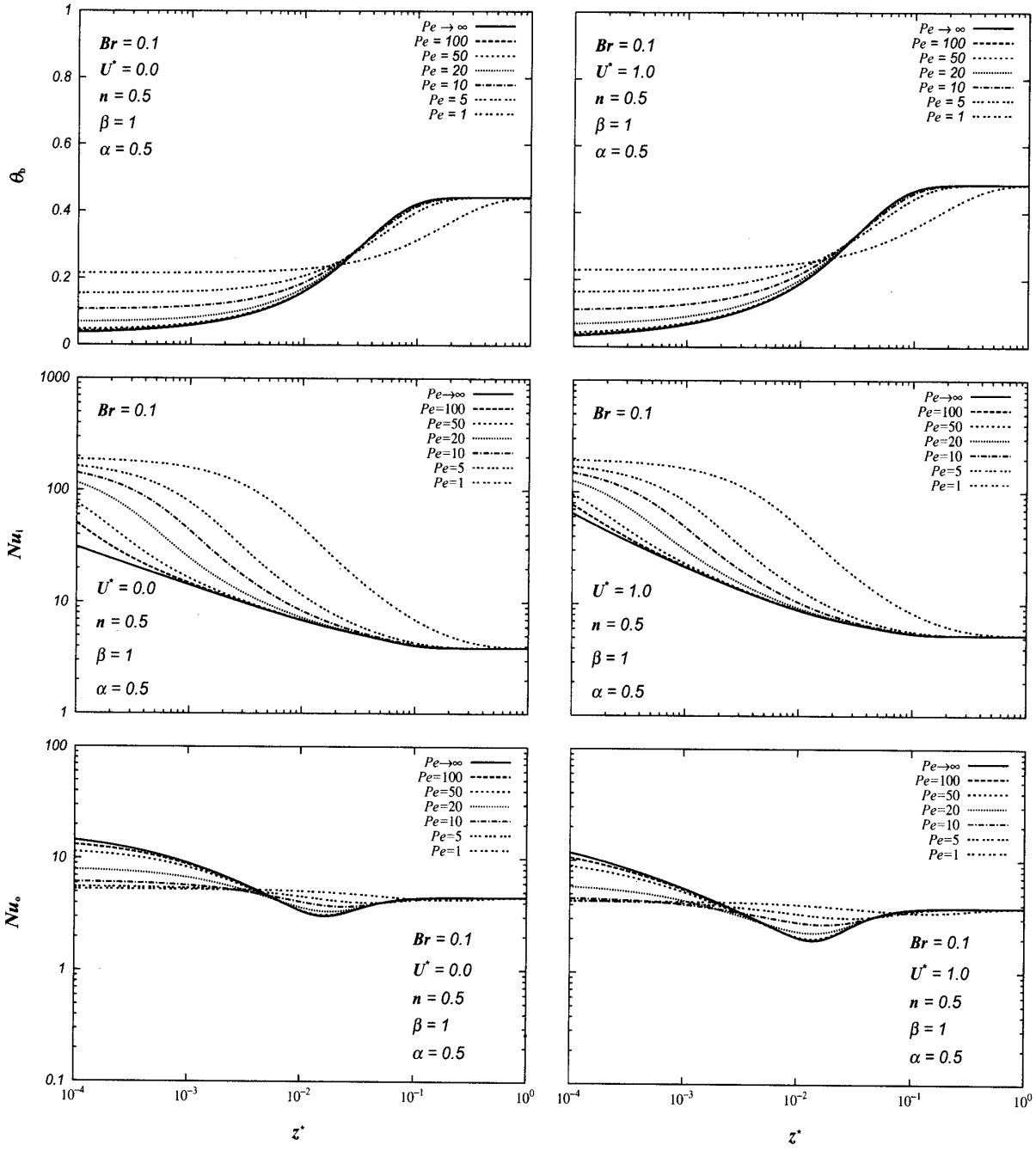

Fig.5 θ_b and Nu for a pseudoplastic fluid, $Br = 0.1$ ($U^* = 0$ and $U^* = 1$)

8, one can see the effects of Br and Pe on Nusselt number for a pseudoplastic fluid and a dilatant fluid respectively. From these figures it is seen, the effect of fluid axial heat conduction accounts for the change in the curve shape in the thermal entrance region. For the stationary core case, Br has a strong effect on Nu in the fully developed region. But Nusselt curves at the core are almost identical for the equal Pe values for the different values of Brinkman number if $U^* = 1$. For $U^* = 0$, Nusselt number at the core decreases with an increase in Brinkman number in the fully developed region.

In order to study the radius ratio effects, heat transfer results are shown in Fig.9. The general behavior was quite similar for different fluids and for various Pe. Therefore as an example, the calculation results for a pseudoplastic fluid are shown for $Pe = 10$. The results indicate that the radius ratio $\alpha = 0.2$ is superior to $\alpha = 0.5$ and $\alpha = 0.8$ from the view point of heat transfer at the core under the same conditions.

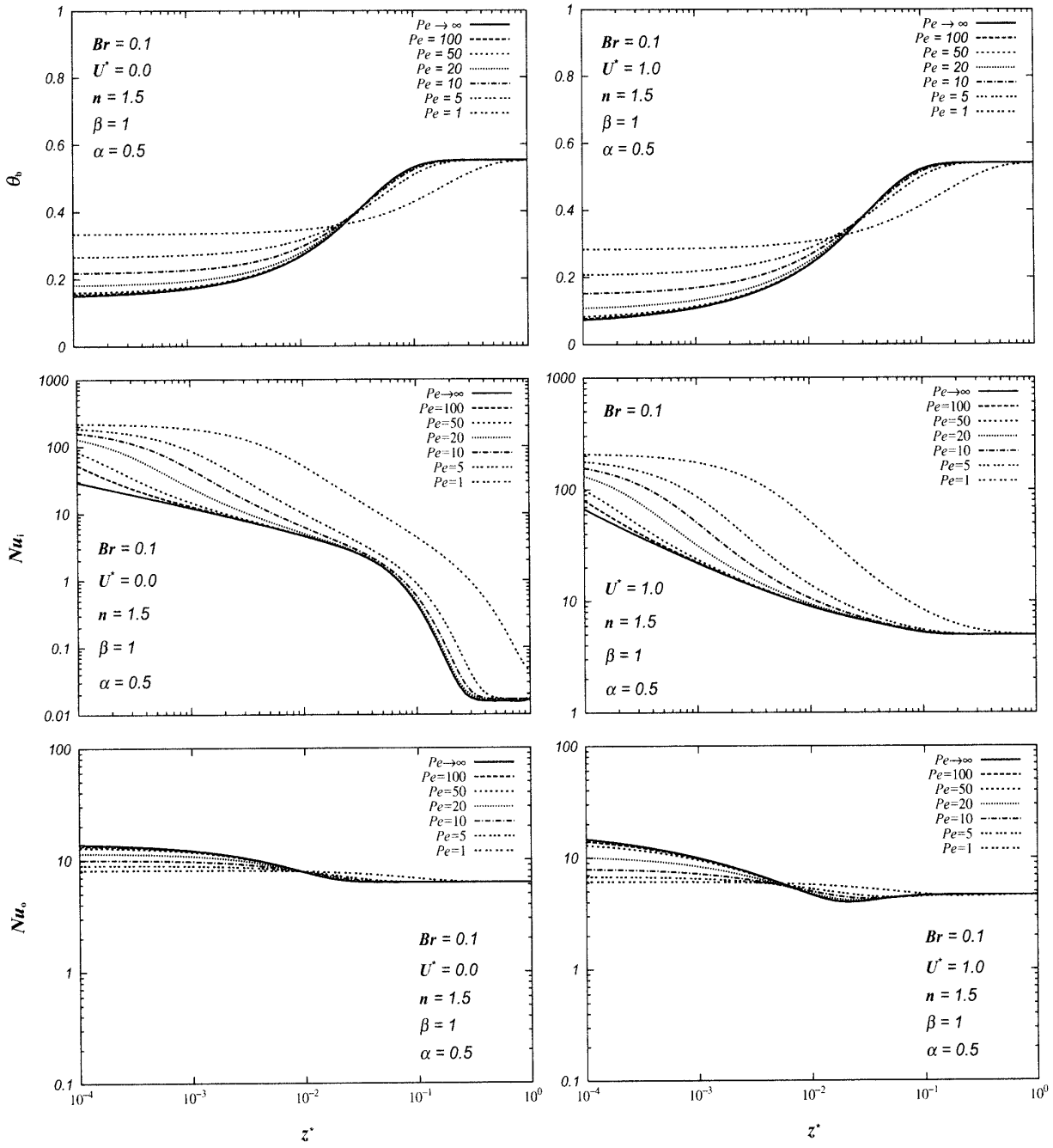

Fig.6 θ_b and Nu for a dilatant fluid, $Br = 0.1$ ($U^* = 0$ and $U^* = 1$)

5. Conclusions

The problem of laminar heat transfer in the thermal entrance region including viscous dissipation of the flowing non-Newtonian fluids and fluid axial heat conduction is analyzed by considering an infinite axial domain with constant wall temperature condition. The results are presented graphically in dimensionless form and the effects of moving boundary, fluid axial heat conduction, viscous dissipation, flow index and radius ratio are mainly demonstrated.

An inspection of the temperature profile development reveals that the fluid temperature increases at $z \leq 0$ due to fluid axial heat conduction and viscous heating. Including the effect of fluid axial heat conduction in the analyses results in higher values for the Nusselt number at the heated core in the thermal region than in the case with neglected axial heat conduction for a given z.

It may be concluded that the effect of fluid axial heat conduction is negligible only at high Pe. For moderate values of Pe number, fluid axial heat

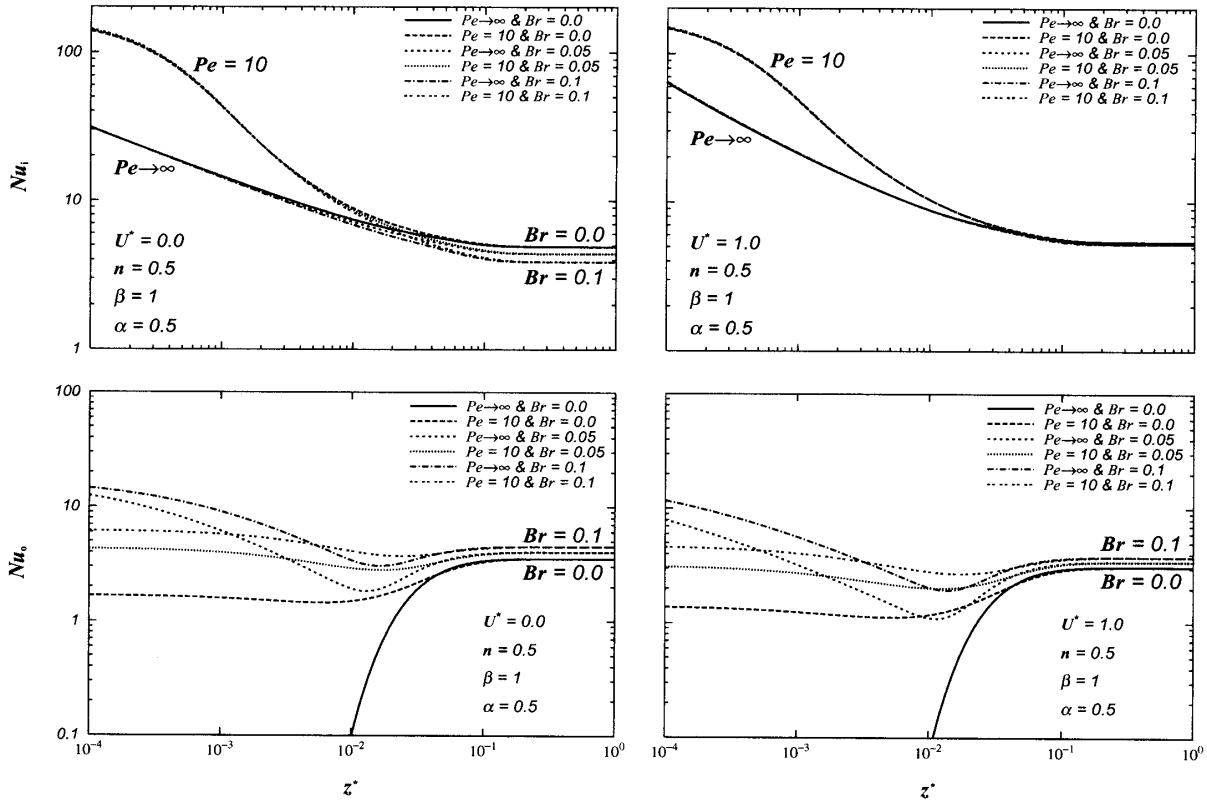

Fig.7 Nu variations for a pseudoplastic fluid with different degrees of viscous dissipation and fluid axial heat conduction ($U^* = 0$ and $U^* = 1$)

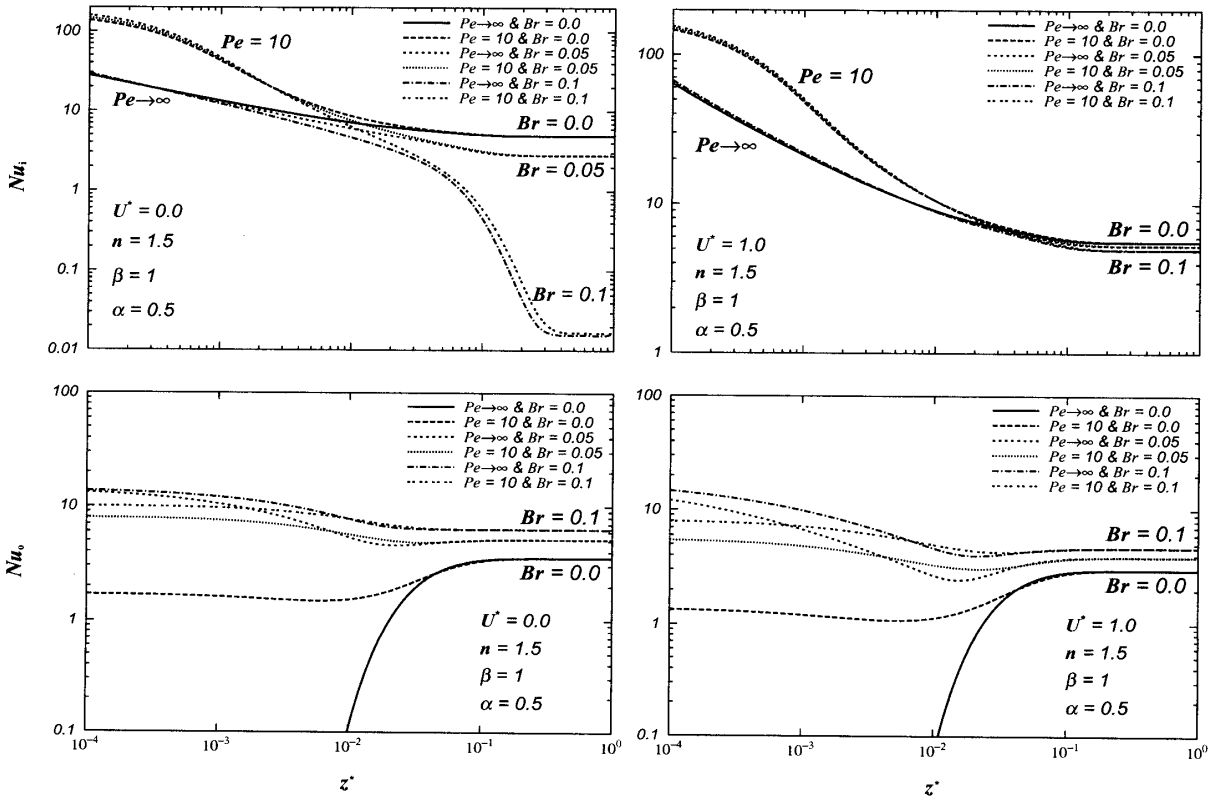

Fig.8 Nu variations for a dilatant fluid with different degrees of viscous dissipation and fluid axial heat conduction ($U^* = 0$ and $U^* = 1$)

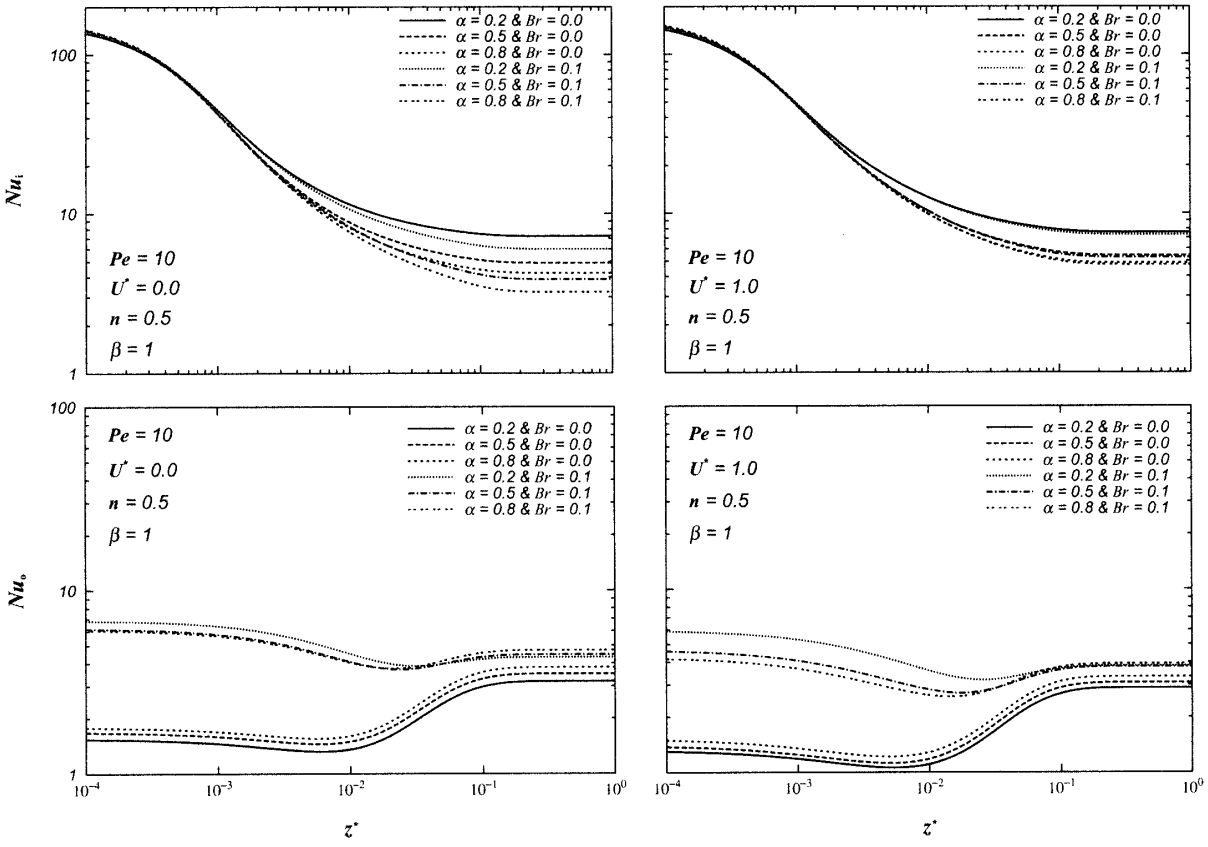

Fig.9 Nu for different α ($U^* = 0$ and 1)

conduction is important at the thermal entrance region. The effect of Br is stronger on Nusselt number at the unheated, fixed tube.

For thermally developing flow when $Br \neq 0$, it is shown that the viscous dissipation effect is different depending on U^*. Nu_i at the the moving heated core ($\theta_\mathrm{i} = 1$) is little sensitive to Br. It was found that the curves for Nu_o at the outer tube ($\theta_\mathrm{o} = 0$) do not change monotonically along the axial distance particularly in the thermally developing region.

The counterpart for the second kind of the boundary condition will be given in the next report.

References

1. Ganbat Davaa, Toru Shigechi and Satoru Momoki, "Laminar Heat Transfer in the Thermal Entrance Region of Concentric Annuli with Moving Heated Cores" (Part I: the first and second kinds of thermal boundary conditions), *Reports of the Faculty of Engineering, Nagasaki University*, vol.32, No.59, 41-50, (2002).
2. Ganbat Davaa, Toru Shigechi and Satoru Momoki, "Fluid Flow for Modified Power Law Fluids in Concentric Annuli with Axially Moving Cores", *Reports of the Faculty of Engineering, Nagasaki University*, vol.32, No.58, 83-90, (2002).
3. S.Kakac, R.K.Shah and W.Aung (eds.), "Handbook of Single-Phase Convective Heat Transfer", *Wiley, New York*, 20.2-20.32, (1987).
4. F.H.Verhoff and D.P.Fisher, "A Numerical Solution of the Graetz Problem with Axial Conduction Included", *Journal of Heat Transfer, Trans. ASME*, vol.95, No.1, 132-134, (1973).
5. R.K.Shah and A.L.London, "Laminar Flow Forced Convection in Ducts", *Advances in Heat Transfer*, Supplement 1, Academic Press, (1970).
6. K.Araki, "Laminar Heat Transfer in Annuli", *Department of Mechanical Engineering, Nagasaki University*, Master Thesis, (1991) (in Japanese).